Optimizing Practical Adaptive Frequency Hopping and Medium Access Control in Ad Hoc Networks

Ralph Tanbourgi, Jens Elsner, Holger Jäkel, Friedrich K. Jondral

Optimizing Practical Adaptive Frequency Hopping and Medium Access Control in Ad Hoc Networks

(Invited Paper)

Ralph Tanbourgi, Jens P. Elsner, Holger Jäkel and Friedrich K. Jondral
Communications Engineering Lab, Karlsruhe Institute of Technology, Germany
Email: {ralph.tanbourgi, jens.elsner, holger.jaekel, friedrich.jondral}@kit.edu

***Abstract*—Adaptive frequency hopping (AFH) as proposed, e.g., in IEEE 802.15.2 aims at increasing system reliability in the presence of quasi-static *external* interference. Practical approaches require autonomous sensing of the interference environment, with the measurements containing both external interference and network *self*-interference. In prior work, a simplistic model for AFH-based ad hoc networks was developed to analyze how this issue affects the area spectral efficiency (ASE). It was found that the AFH mechanism severely degrades ASE when self-interference is increased. In this paper, we modify the model to account for the correlation between the nodes' adapted hop sets. We then address the question of how to design the system parameters to achieve optimal performance and avoid the degradation. We discuss different optimization problems and identify sensing techniques that can cope with increased self-interference. Among these techniques, carrier detection sensing was found to be robust against self-interference while showing good performance. We further discuss cases where joint optimization of the AFH and CSMA mechanisms is beneficial and cases where there is little to be gained.**

***Index Terms*—Adaptive frequency hopping, interference, ad hoc networks, area spectral efficiency, stochastic geometry.**

I. Introduction

In dense wireless ad hoc networks, interference is the limiting factor to performance in most cases. One has to differentiate between *self*-interference, created by devices using the same transmission standard, and *external* interference, created by co-located other systems operating in the same spectrum. In order to reduce link outages due to self-interference, frequency hopping (FH) was found promising [1]. Carrier sense multiple access (CSMA) can additionally be employed as medium access control (MAC) scheme to inhibit close-by transmissions [2], and hence to avoid excessive self-interference.

To counteract external interference, a co-existence approach named *adaptive frequency hopping* (AFH) was proposed in [3] for systems operating in non-regulated spectrum. AFH adapts the hop set, i.e, the channels used for hopping, such that channels polluted by external interference are excluded from the hop set. Practical AFH uses a channel sensing technique based on, e.g., received signal strength, packet error rate or carrier detection, for detecting external interference.

Both the CSMA and the AFH mechanism can be optimized in a straightforward way, when either self-interference or external interference is neglected. However, separate optimization does not yield global optimality in general, as the mutual influence of the two mechanisms is omitted. This poses a problem, especially when considering future applications of wireless personal/local area networks (WPANs/WLANs), where performance will often be limited by both types of interference without one type dominating the other [4].

To highlight this issue, we derived in [5] a model for AFH that is based on stochastic geometry and that takes into account the mutual influence between the CSMA and the AFH mechanism. It was shown that practical AFH with imperfect/practical sensing, i.e., when the AFH sensing measurements contain not only external interference but also self-interference, can result in adverse behavior of AFH when self-interference increases. The problem of how to properly adjust the sensing mechanism is even further aggravated by the fact that the parametrization is not standardized and remains vendor-specific.

In this paper, we will extend the work in [5] in order to

- account for the correlation between the adapted hop sets of the nodes,
- obtain the ASE of properly optimized practical AFH,
- compare different AFH sensing techniques and,
- answer the question "When do adaptive thresholds outperform static thresholds?".

II. Network Model

A packet-based FH wireless network with m orthogonal channels consists of nodes distributed in $\mathbb{R}^2$. We assume slotted medium access. A *guard zone* (cf. [2]) is employed by the receivers to avoid excessive self-interference. The guard zone (GZ) is an appropriate model for CSMA with request-to-send (RTS) and clear-to-send (CTS) handshake, since close-by transmissions around a receiver are inhibited. We further assume a fixed transmission power ρ for all nodes.

A. Interference model and AFH mechanism

Self-interference is assumed to be fast-varying (on the order of the slot length) due to alternating transmitter/receiver (Tx/Rx) roles and possibly mobility. The nodes also experience external interference: The received external interference powers $\mathsf{n}_1, \ldots, \mathsf{n}_m$ are identically distributed at each node and independent and identically distributed (i.i.d.) for each channel. The realizations $n_1, \ldots, n_m$ are quasi-static.

All nodes employ AFH with a fixed sensing threshold θ. The set of active channels (hop set) of a node depends solely on this node's view on the interference, i.e., nodes do not coordinate their decisions about their hop set. To satisfy

978-1-61284-824-2/2012 - Copyright is with IFIP

regulatory spectrum masks, the number of active channels in a node's hop set is never less than k. We denote by $\mathsf{v} \in [k, m]$ the total number of active channels in the network. We assume that the hopping sequences always remain pseudo-random.

B. Traffic and channel model

In a given slot, some nodes decide to transmit. The positions of these nodes are assumed to form a stationary Poisson point process (PPP) of intensity λ_b. When accessing the medium, each of these potential Txs tunes to a channel ℓ corresponding to the (adapted) hop set of the intended Rx. We assume that all Txs have their intended Rx situated at fixed (target) distance d. Only those potential Txs not inhibited by the GZ mechanism are allowed to transmit.

The path loss between two arbitrary positions x, y is given by $\|x-y\|^{-\alpha}$, where $\alpha > 2$ is the path loss exponent. We assume i.i.d. Rayleigh fading between the nodes in the network, while for the channels from external sources to the nodes we do not make any specific assumption. The power fading between a Tx at x and an Rx at y is given by g_{xy}, which follows a unit-mean exponential distribution. The (possible) power fading between external source and an Rx at y is h_y.

C. Probe link and guard zone model

We consider a *probe* link in channel ℓ with an Rx placed in the origin o and an associated Tx placed $d > 1$ units away at $z \in \mathbb{R}^2$. The restriction $d > 1$ guarantees the validity of the path loss model. We define by $\mathsf{u} \in [k, m]$ the number of active channels of the probe Rx. Since both the Tx set and the Rx set are stationary, the probe link is *typical* for the network, cf. [6]. Considering u as a mark attached to the probe Rx, u can be seen as the typical mark, cf. [7].

We use an approximation technique similar to [8] to model the GZ mechanism. First, the *large-scale density* of Txs in channel ℓ is derived using the fact that the Txs inhibited by the GZs of the Rxs can be seen as a Matérn-*like* point process, cf. [8]. Then, using [9] the large-scale density in an *active* channel ℓ, when $\mathsf{v} = v$ channels are active in the network, is

$$\lambda_\ell(v) := \frac{\lambda_\mathsf{b}}{v} \frac{1-\exp(-N)}{N}. \tag{1}$$

N is the average number of Rxs in the contention set of the probe Tx which reflects the average number of MAC contentions of a typical link. An Rx is in the contention set of the probe Tx, if the probe Tx senses the CTS beacon of this Rx, where γ is the associated GZ sensing threshold. In (1), we have implicitly assumed that the density λ_b is "equally distributed" over all v active channels. The considered scenarios introduced in III-B will satisfy this restriction. For an *inactive* channel ℓ, we write $\lambda_\ell(v) = 0$. We denote by $\lambda(v) = \sum_{\ell=1}^{m} \lambda_\ell(v)$ the *total large-scale density* in the network, given $\mathsf{v} = v$ active channels. From the "equally distributed"-property, we have that $\lambda_\ell(v) = \lambda(v)/v$ for every *active* channel. We will use this notation throughout the paper. N can be calculated as [8]

$$N = \int_{\mathbb{R}^2} \frac{\lambda_\mathsf{b}}{v} e^{-\frac{\gamma}{\rho}\|x\|^\alpha} \mathrm{d}x = \frac{\lambda_\mathsf{b}}{v} \pi \Gamma(1+\tfrac{2}{\alpha}) \left(\frac{\rho}{\gamma}\right)^{\frac{2}{\alpha}}, \tag{2}$$

where $\Gamma(a) := \int_0^\infty t^{a-1} e^{-t}\,\mathrm{d}t$ is the Gamma function.

Secondly, the interference field at the probe receiver is modeled using a non-homogeneous PPP approximation capturing the *shot-range inhibition*. With this approximation, the Txs in the same channel ℓ around o follow a PPP $\Phi_\ell := \{\mathsf{x} : \mathsf{x} \in \mathbb{R}^2\}$ of intensity $(1-\exp(-\gamma\|x\|^\alpha/\rho))\,\lambda(v)/v$. The term $1-\exp(-\gamma\|x\|^\alpha/\rho)$ can be seen as the thinning probability of a *position-dependent thinning*, cf. [8].

III. Area Spectral Efficiency of AFH

We now briefly introduce the performance metrics required for the optimization and recall some results from [5].

A. Performance metrics

Interference is treated as white noise at the decoder and thermal noise is neglected. The signal-to-interference ratio (SIR) in channel ℓ at the probe Rx is then given by

$$\mathsf{SIR}_\ell := \frac{\rho \mathsf{g}_{zo} d^{-\alpha}}{\mathsf{h}_o \mathsf{n}_\ell + \sum\limits_{\mathsf{x}\in\Phi_\ell\setminus\{z\}} \rho \mathsf{g}_{\mathsf{x}o} \|\mathsf{x}\|^{-\alpha}} = \frac{\mathsf{g}_{zo}}{\mathsf{h}_o \eta_\ell + \mathsf{Y}_\ell}, \tag{3}$$

where $\eta_\ell := \frac{\mathsf{n}_\ell d^\alpha}{\rho}$ and $\mathsf{Y}_\ell := d^\alpha \sum_{\mathsf{x}\in\Phi_\ell\setminus\{z\}} \mathsf{g}_{\mathsf{x}o}\|\mathsf{x}\|^{-\alpha}$ are the normalized external and self-interference power in o. The distribution of η_ℓ and n_ℓ is identical except for scaling. Unless stated otherwise, we set $\rho = 1$ without loss of generality.

The outage probability (OP) of the probe link in channel ℓ, given $\mathsf{v} = v$ active channels in the network, is the probability that SIR_ℓ is below a modulation/coding specific threshold β,

$$q(\lambda(v)/v, \eta_\ell) := \mathbb{P}^{!z}\left(\mathsf{SIR}_\ell < \beta\right), \tag{4}$$

where $\mathbb{P}^{!z}$ refers to the reduced Palm probability [9]. The argument v in (4) indicates that the OP depends on the number of active channels in the network via the intensity of Φ_ℓ. As shown in [5], equation (4) can be computed as

$$q(\lambda(v)/v, \eta_\ell) = 1 - \mathcal{L}_{\mathsf{h}_o}(\beta\eta_\ell)\,\Omega(v), \tag{5}$$

where $\mathcal{L}_{\mathsf{h}_o}(\cdot)$ is the Laplace transform of h_o,

$$\Omega(v) := \exp\left(\frac{-2\pi^2\lambda(v)s^{\frac{2}{\alpha}}}{v\alpha\sin\frac{2\pi}{\alpha}}\left[1 - e^{\gamma s}\frac{\Gamma(1-\frac{2}{\alpha},\gamma s)}{\Gamma(1-\frac{2}{\alpha})}\right]\right), \tag{6}$$

and $s := \beta d^\alpha$. $\Gamma(a,b) := \int_b^\infty t^{a-1}e^{-t}\,\mathrm{d}t$ is the upper incomplete Gamma function.

Remark 1. For $\gamma \to \infty$, we have $\Omega(v) \to \exp(\frac{-2\pi^2\lambda(v)s^{2/\alpha}}{v\alpha\sin 2\pi/\alpha})$ in (6) which constitutes the OP for slotted Aloha. This is consistent with the observation in [8].

The area spectral efficiency (ASE) Υ is defined as the average aggregated per channel large-scale density weighted by the probability of success of the probe link, i.e.,

$$\Upsilon := \mathbb{E}_{\mathsf{v},\eta_1,\ldots,\eta_m}\left[\sum_{\ell=1}^{m} \lambda_\ell(\mathsf{v})\left(1 - q\left(\tfrac{\lambda(\mathsf{v})}{\mathsf{v}}, \eta_\ell\right)\right)\right]. \tag{7}$$

Here, we average over the external interference, which influences the large-scale density through v on the one hand, and the OP of the probe link through $\eta_1, \ldots, \eta_m$ on the other.

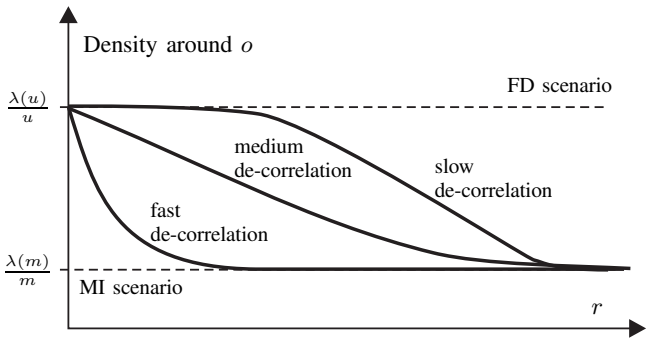

Fig. 1. SC scenario: The density of interferers in an active channel around the probe receiver in o. Different types of decay for $c(r)$ are illustrated.

The ASE will strongly depend on *how the nodes are affected* by external interference, cf. [5]. Next, three scenarios, each with a different view on external interference, are introduced.

B. Reference scenarios

1) Full dependence (FD) scenario: In the FD scenario all nodes observe the same realization $n_1, \ldots, n_m$, and thus will discard the same channels. Hence, the set of active channels (of the probe receiver) is the same for all nodes, implying $\mathsf{v} \equiv \mathsf{u}$. The large-scale density in each *active* channel is therefore $\lambda(\mathsf{v})/\mathsf{v} \equiv \lambda(\mathsf{u})/\mathsf{u}$. This scenario models the case where nodes form close-by piconets and the external system is far away.

2) Mutual independence (MI) scenario: In the MI scenario, every node sees its own realization $n_1, \ldots, n_m$. Thus, the sets of active channels are independent among the nodes. Since the $\mathsf{n}_1, \ldots, \mathsf{n}_m$ are i.i.d., the load in each channel should remain the same, implying $\mathsf{v} \equiv m$ almost sure (a.s.). As a result, the large-scale density is $\lambda(m)/m$ in *each* channel.

3) Spatial correlation (SC) scenario: While the FD and MI scenario represent the two extreme cases, the SC scenario models a more realistic semi-dependent case, where close-by nodes experience the same external interference and external interference de-correlates with distance.

For modeling such a scenario, we assume a generic *de-correlation function* $0 \leq c(r) \leq 1$ which characterizes the correlation of the hop sets of two receivers y_1, y_2 separated by r units. Clearly, $c(0) = 1$ and $\lim_{r\to\infty} c(r) = 0$. When averaged over all spatial configurations, the distance between two receivers y_1, y_2 is approximately the same as the distance between receiver y_1 and the intended transmitter of receiver y_2. Thus, from the viewpoint of the probe receiver having $\mathsf{u} = u$ active channels, the density of interferers in the same active channel at distance r is approximately $c(r)(\lambda(u)/u - \lambda(m)/m) + \lambda(m)/m$, cf. Fig. 1. Recall that the large-scale density is the density "seen from far away". Hence, if $\lim_{r\to\infty} c(r) = 0$ (arbitrarily slow), the large-scale density in this scenario is $\lambda(m)/m$ in each channel as for the MI scenario. Such a scenario could be constructed by overlaying an additional network with (legacy) users independently selecting a channel at random (each with probability $1/m$).

Lemma 1. For $0 \leq v \leq m$, $\lambda(m) \geq \lambda(v)$ with equality only for $v = m$.

Proof: Combining (1) and (2) we have to show that

$$\frac{m(1-e^{-\frac{b}{m}})}{v(1-e^{-\frac{b}{v}})} \geq 1 \quad \forall m \geq v, \tag{8}$$

where $b = \lambda_{\mathsf{b}}\pi\Gamma(1+\frac{2}{\alpha})\gamma^{-\frac{2}{\alpha}} > 0$. This is equivalent to showing that $m(1-e^{-\frac{b}{m}})$ is non-decreasing in m for all $b > 0$:

$$\frac{\partial\, m(1-e^{-\frac{b}{m}})}{\partial\, m} = 1 - (1+\tfrac{b}{m})e^{-\frac{b}{m}} > 1 - \underbrace{(1+\tfrac{b}{m}+\tfrac{b^2}{2m^2}+\ldots)}_{e^{\frac{b}{m}}} e^{-\frac{b}{m}} = 0 \quad \blacksquare$$

C. ASE with perfect sensing

We start the analysis by considering the ASE for AFH with perfect sensing. The ASE for imperfect sensing will follow from these observations. From [5], the ASE Υ for the FD scenario ($\mathsf{v} \equiv \mathsf{u}$) with perfect sensing is given by

$$\Upsilon^{\mathrm{FD}} = \lambda(k)\,\Omega(k) \int_\theta^\infty \mathbb{E}_{\mathsf{\eta}}\left[\mathcal{L}(\beta\mathsf{\eta})\,|\mathsf{\eta} \leq t\right] \mathrm{d}\mathbb{P}\left(\mathsf{\eta}_{(k+1)} = t\right) + \mathbb{E}_{\mathsf{\eta}}[\mathcal{L}_{\mathsf{h}_o}(\beta\mathsf{\eta})\,|\mathsf{\eta} \leq \theta] \sum_{u=k+1}^{m} \lambda(u)\,\Omega(u)\,\mathbb{P}\left(\mathsf{u} = u\right), \tag{9}$$

and, similarly, for the MI scenario ($\mathsf{v} \equiv m$)

$$\Upsilon^{\mathrm{MI}} = \lambda(m)\,\Omega(m) \Bigg[\int_\theta^\infty \mathbb{E}_{\eta}\left[\mathcal{L}(\beta\eta)\,|\eta \leq t\right] \mathrm{d}\mathbb{P}\left(\eta_{(k+1)} = t\right) + \mathbb{E}_{\eta}[\mathcal{L}_{H_0}(\beta\eta)\;|\eta \leq \theta] \left(\mathbb{P}(\mathsf{u} \leq m) - \mathbb{P}(\mathsf{u} = k)\right) \Bigg], \tag{10}$$

where $\mathsf{\eta}_{(i+1)}$ is the $(i+1)$-th order statistic of $\mathsf{\eta}_1, \ldots, \mathsf{\eta}_m$ and

$$\mathbb{P}\left(\mathsf{u} = u\right) = \begin{cases} \mathbb{P}\left(\mathsf{\eta}_{(k+1)} > \theta\right), & u = k \quad (11a) \\ \mathbb{P}\left(\mathsf{\eta}_{(u)} \leq \theta, \mathsf{\eta}_{(u+1)} > \theta\right), & k < u < m \quad (11b) \\ \mathbb{P}\left(\mathsf{\eta}_{(m)} \leq \theta\right), & u = m. \quad (11c) \end{cases}$$

The next result relates the FD scenario to the MI scenario for the limiting cases.

Theorem 1. When the network is not limited by external interference ($\rho \to \infty$), it follows that $\mathcal{L}_{\mathsf{h}_o}(\beta\mathsf{\eta}_\ell) \equiv 1$ for all ℓ and $\mathsf{u} \equiv \mathsf{v} \equiv m$ a.s., and hence $\Upsilon^{\mathrm{FD}} = \Upsilon^{\mathrm{MI}} = \lambda(m)\Omega(m)$.

When the network is mainly limited by external interference ($\rho \to 0$), $\mathsf{v} \equiv m$ for the MI scenario and $\mathsf{v} \equiv k$ for the FD scenario a.s.. Furthermore, $\mathcal{L}_{\mathsf{h}_o}(\beta\mathsf{\eta}_\ell) \equiv 0$ for all ℓ a.s., and hence $\Upsilon^{\mathrm{FD}}, \Upsilon^{\mathrm{MI}} \to 0$, with $\Upsilon^{\mathrm{FD}}/\Upsilon^{\mathrm{MI}} = \frac{\lambda(k)\Omega(k)}{\lambda(m)\Omega(m)}$.

Proof: The two statements follow by simply considering the effect of the AFH mechanism on the hop set for the two extreme cases $\rho \to \infty$ and $\rho \to 0$. $\blacksquare$

Lemma 2. The success probability Ω^{SC} with respect to outage due to the self-interference in the SC scenario is

$$\Omega^{\mathrm{SC}}(u) = \exp\left[-2\pi s \left(\frac{\lambda(u)}{u} - \frac{\lambda(m)}{m}\right) A\right] \Omega(m), \tag{12}$$

where $A := \int_0^\infty \frac{1-e^{-\gamma r^\alpha}}{s+r^\alpha} r c(r)\,\mathrm{d}r$ and $s = \beta d^\alpha$.

Proof: The OP for Aloha MAC and Rayleigh fading can be computed using standard methods (i.e., conditioning of Φ_ℓ and applying the definition of the Laplace functional for a

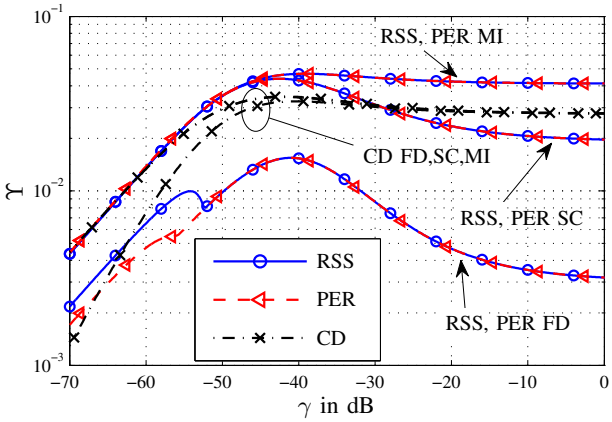

Fig. 2. ASE Υ vs. γ for RSS, PER, CD sensing. Parameters are: $m = 79$, $k = 20$, λ_b, $\alpha = 4$, $d = 10$, $\beta = 2$, $\theta_\mathrm{r} = -12$ dB, $\theta_\mathrm{p} = 5$ %, $\theta_\mathrm{c} = 10$ dB. The $\eta_1, \ldots, \eta_m$ follow a log-normal distribution with $\mu = -14$ dB and $\sigma = 16$ dB. No fading between external source and the nodes ($\mathsf{h}_o \equiv 1$).

PPP), cf. [7]. We only have to substitute the large-scale density of Φ_ℓ by $c(r)(\lambda(u)/u - \lambda(m)/m) + \lambda(m)/m$. ∎

The expression in (12) has an interesting interpretation: the term Ω^{SC} can be written as the product of the success probability $\Omega(m)$ for the MI scenario and a correction term that is related to the FD scenario. This correction term depends on the specific form of the function $c(r)$. The OP for the FD and MI scenarios can be seen as special cases of (12):

1) FD: $c(r) = 1$: In this case, $\mathsf{v} \equiv \mathsf{u}$ and $\Omega^{\mathrm{SC}}(u) = \Omega(u)$.
2) MI: $c(r) = 0$: In this case, $A = 0$ and $\Omega^{\mathrm{SC}}(u) = \Omega(m)$.

Note that in 1), we have to set the large-scale density to $\lambda(u)/u$ in addition to $c(r) = 1$ (full dependence of the hop set).

Theorem 2. The ASE for the three scenarios FD, MI and SC satisfy the following ordering

$$\Upsilon^{\mathrm{FD}} \leq \Upsilon^{\mathrm{SC}} \leq \Upsilon^{\mathrm{MI}}. \tag{13}$$

Proof: Lower bound (FD): For $\lim_{r\to\infty} c(r) = 0$, the dependence of the hop sets of two largely separated nodes is vanishing. Thus we have $\lambda(m)$ as total large-scale density which is greater than $\lambda(u)$ by Lemma 1. Furthermore, since $c(r) \leq 1$, the intensity of interferers around the probe receiver is never greater than in the FD case, and thus $\Omega^{\mathrm{SC}}(u) \geq \Omega(u)$. Upper bound (MI): The large-scale density for the MI and SC scenario are the same. Furthermore, we have $A \geq 0$ since $c(r) \geq 0$ and also $\frac{\lambda(u)}{u} - \frac{\lambda(m)}{m} \geq 0$. Thus, $\Omega^{\mathrm{SC}}(m)$ in (12) is bounded above by $\Omega(m)$. Pair-wise equality holds for the cases 1) and 2) shown above. ∎

D. Effect of imperfect sensing

Practical AFH requires the nodes to sense the external interference on their own. This sensing process is in general *imperfect*, meaning that external interference cannot be know perfectly due to the (additive) presence of self-interference in the sensing measurements. In practice, the measurements are usually averaged over time to obtain long-term observations and to average out fluctuations caused by self-interference (Y) and fading (h_o). We assume that the averaging is sufficiently long so that all fluctuations disappear. We now introduce three commonly used sensing methods.

1) Received signal strength (RSS): RSS measurements can be used to detect a co-located system. By measuring the RSS when being idle, a node can obtain the channel qualities. When normalized to the average received power, the measurement $\eta_\ell + \mathbb{E}[\mathsf{Y}_\ell]$ in channel ℓ is compared to a threshold θ_r.

2) Packet error rate (PER): This method implicitly measures the channel qualities by estimating the PER and comparing it to a threshold θ_p. With a sufficiently large averaging period, the measurement will converge to the OP from (5).

3) Carrier detection (CD): CD can be used to robustly detect signals from external systems. We assume that a node performs the sensing process when it is in idle mode. Since the signal to be detected is superimposed with FH signals, the detection process in channel ℓ is successful only if the ratio $\frac{\eta_\ell}{\mathbb{E}[\mathsf{Y}_\ell]}$ is above a certain threshold θ_c.

For the MI and FD scenario, the normalized average self-interference $\mathbb{E}[\mathsf{Y}(v)]$ measured in an active channel, given $\mathsf{v} = v$, can be calculated using Campbell's Theorem [9] as

$$\mathbb{E}[\mathsf{Y}(v)] = \frac{2\pi\lambda(v)d^\alpha}{v(\alpha-2)}\gamma^{1-\frac{2}{\alpha}}\Gamma\left(\tfrac{2}{\alpha}\right), \quad \text{for FD and MI.} \tag{14}$$

Similarly, $\mathbb{E}[\mathsf{Y}(v)]$ in an active channel for the SC scenario can be computed as

$$\mathbb{E}[\mathsf{Y}(u)] = \mathbb{E}[\mathsf{Y}(m)] + d^\alpha\left(\tfrac{\lambda(u)}{u} - \tfrac{\lambda(m)}{m}\right) \times 2\pi\int_0^\infty c(r)\, r^{-\alpha+1}\left(1 - e^{-\gamma r^\alpha}\right)\mathrm{d}r, \quad \text{for SC.} \tag{15}$$

The key idea for calculating the ASE with imperfect sensing is to isolate η_ℓ from the self-interference part in the measurements of the active channels. In equilibrium,[1] the resulting modified thresholds for the active channels are then given by

$$\theta(v) = \begin{cases} \theta_\mathrm{r} - \mathbb{E}[\mathsf{Y}(v)], & \text{for RSS} \quad (16a) \\ \frac{1}{\beta}\log\frac{\Omega(v)}{1-\theta_\mathrm{p}}, & \text{for PER} \quad (16b) \\ \theta_\mathrm{c}\mathbb{E}[\mathsf{Y}(v)], & \text{for CD.} \quad (16c) \end{cases}$$

Remark 2. The thresholds in (16) now depend on v through $\mathbb{E}[\mathsf{Y}(v)]$ (RSS, CD) and $\Omega(v)$ (PER). Recall that for the FD and SC scenario,[2] $\mathsf{v} \equiv \mathsf{u}$ and for the MI scenario, $\mathsf{v} \equiv m$ a.s.

Fig. 2 shows the basic behavior of the ASE Υ vs. γ for the different sensing methods. It can be seen that the ASE of practical AFH highly depends on the underlying scenario: with increasing dominance of the self-interference (MI→SC→FD), the ASE becomes low, especially for large γ. This is because self-interference, which increases with γ, increases the background interference level, thereby triggering the AFH mechanism to remove more channels. As a result, the interference avoidance feature of FH is reduced, resulting in an ASE drop. For the SC scenario, the function $c(r) = 1/\sqrt{1+r}$ (slow de-correlation) was chosen as an example. It can be seen how the correlation of the hop sets affects the ASE as the self-interference increases.

[1] I.e., when all nodes have adapted their hop set.
[2] Locally, the SC scenario behaves similar to the FD scenario.

IV. Optimization of AFH

Throughout this section, we will use as an example the parameters $m = 79$ and $k = 20$, as they are currently employed in the IEEE 802.15.2 standard [3]. Furthermore, we will treat the case $\mathsf{h}_o \equiv 1$ only, noting that additional fading does not change the results significantly, but may be exploited in some cases [10]. We assume that the $\eta_1, \ldots, \eta_m$ are log-normally distributed ($\log \mathcal{N}(\mu, \sigma^2)$) which additionally accounts for possible shadowing effects.

A. Optimization of guard zone parameter γ

We first start with an optimization of the GZ threshold γ in the absence of external interference (e.g., when $\rho \to \infty$). In this case, the (total) number of active channels is $\mathsf{v} \equiv \mathsf{u} \equiv m$ a.s.. A similar optimization problem was considered in [2], where the optimal (geometric) exclusion radius was derived for the path loss only model.

Optimization problem 1:

$$\gamma^* = \arg\max_{\gamma} \{\lambda(m)\,(1 - q\,(\lambda(m)/m, 0))\} \tag{17}$$

Fig. 3 shows the ASE as well as the optimal threshold γ^* for different transmitter densities λ_b. It can be seen that optimizing over the GZ threshold yields considerable gains compared to sub-optimal γ, particularly in the dense regime. In the low density regime, optimizing over γ does not increase the ASE.

Theorem 3. In the high density regime, the optimal threshold γ^* can be approximated as

$$\gamma^* \approx \frac{1}{d^\alpha \beta} \left(\frac{\alpha}{\pi} \Gamma(1 + 2/\alpha) \sin \tfrac{2\pi}{\alpha} \right)^{\frac{\alpha}{2}}. \tag{18}$$

Proof: In the high density regime, the per channel large-scale density in (1) can be approximated as $\lambda(m)/m \approx \gamma^{2/\alpha}(\pi\Gamma(1 + \frac{2}{\alpha}))^{-1}$ using (2), thereby removing the dependence on λ_b. This behavior can be observed in Fig. 3 for high λ_b. Similarly, we simply approximate the inner brackets of $\Omega(m)$ in (6) by the fixed value 0.5, noting that the true value is between 0 and 1. Combining these two approximates yields

$$\Upsilon \approx \frac{m\gamma^{\frac{2}{\alpha}}}{\pi\Gamma(1 + 2/\alpha)} \exp\left(-\gamma^{\frac{2}{\alpha}} \frac{\pi s^{\frac{2}{\alpha}} \csc \frac{2\pi}{\alpha}}{\alpha\,\Gamma(1 + 2/\alpha)} \right), \tag{19}$$

Setting the derivative of (19) with respect to γ equal to zero and solving for γ yields (18). ∎

For the scenario depicted in Fig. 3, (18) yields $\gamma^* \approx -42.3$ dB which is fairly close to the true value ($\gamma = -45.3$ dB). The loss in ASE due to the approximation is only marginal.

Remark 3. The statements made for the high density regime should be treated with care, since the Poisson approximation becomes inaccurate in this regime. The expressions should be verified by simulations to fine-tune γ^*. However, since in the low and moderate density regime the ASE is nearly invariant to γ, (18) can be used as a near-to-optimal value.

The optimization problem (17) may not be suitable for certain types of applications, e.g., delay-intolerant applications, since no constraints on the OP are made. A more practical optimization problem is given by *Optimization problem 2:*

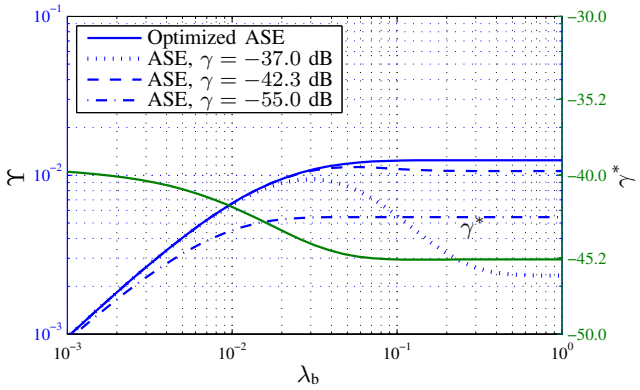

Fig. 3. ASE Υ vs. λ_b for $\alpha = 3$, $d = 14$, $\beta = 4$. No external interference.

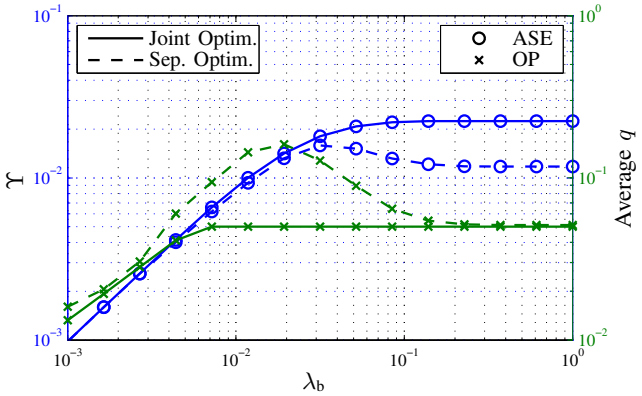

Fig. 4. ASE Υ and average OP q vs. λ_b with PER sensing. Parameters are: $\lambda_\mathrm{b} = 0.1$, $\alpha = 4$, $\beta = 2$, $d = 10$, $\theta_\mathrm{p} = 5$ %, $\mu = -14$ dB and $\sigma = 16$ dB.

$$\gamma^* = \arg\max_{\gamma} \{\lambda(m)\,(1 - q\,(\lambda(m)/m, 0))\} \tag{20a}$$

$$\text{subject to } q\,(\lambda(m)/m, 0) \leq \epsilon. \tag{20b}$$

While the OP constraint ϵ is satisfied, this comes at the cost of reducing ASE (by a factor of 2 compared to Fig. 3).

B. Separate vs. joint optimization

We now consider *Optimization problem 3:*

$$(\theta^*, \gamma^*) = \arg\max_{\theta,\gamma} \Upsilon \tag{21a}$$

$$\text{s.t. } \mathbb{E}_{\mathsf{v},\eta_\ell}\left[q(\lambda(\mathsf{v})/\mathsf{v}, \eta_\ell)\right] \leq \epsilon, \tag{21b}$$

which jointly maximizes the ASE Υ over γ and θ subject to an OP constraint ϵ. Note that ϵ in fact refers to the OP averaged over η of an active channel ℓ,[3] implying that the OP requirement must be satisfied on average. Note that (21) strongly resembles the transmission capacity [6], except that the OP constraint as well as the maximum density of concurrent Txs are averaged over the external interference.

Fig. 4 shows the optimization result for PER sensing with a target OP of 5%. The dashed curves show the performance when the GZ and AFH mechanisms are optimized separately, i.e., γ^* is used in combination with a conservatively chosen

[3]It suffices to consider only one active channel ℓ due to distributional equivalence of the active channels of the (probe) Rx.

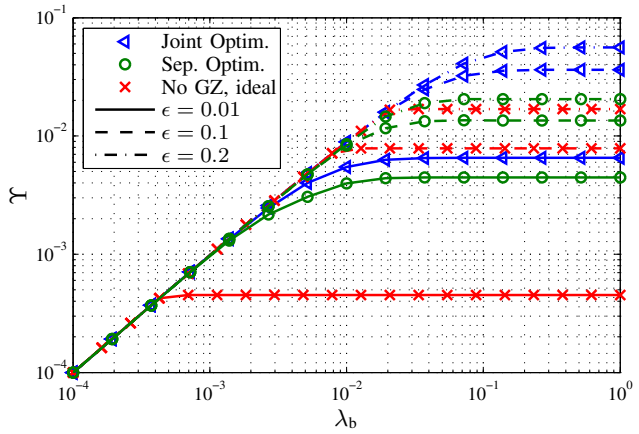

Fig. 5. ASE Υ for optimized practical AFH with GZ and ideal AFH without GZ for different OP constraints ϵ. Parameters are: $\alpha = 4$, $d = 10$, $\beta = 4$.

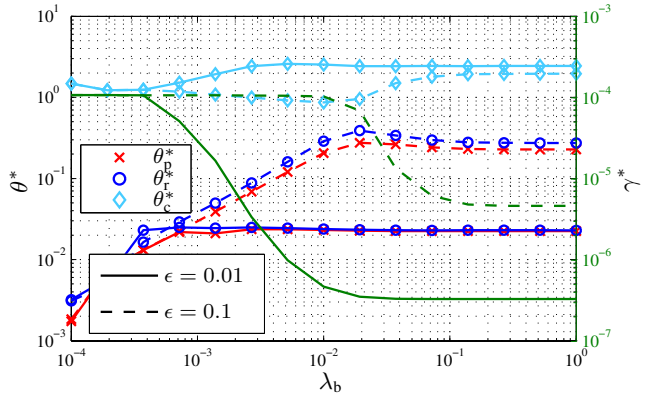

Fig. 6. Optimal θ^*, γ^* vs. λ_b for different OP ϵ and $\alpha = 4$, $d = 10$, $\beta = 4$.

AFH threshold θ. It can be seen that joint optimization yields considerable gains in terms of ASE (up to two times) and average OP (up to three times). Furthermore, the target OP cannot be achieved in the case of separate optimization.

The ASE of optimized practical AFH is shown in Fig. 5 for the FD scenario and different ϵ. The ASE results are the same for all optimized sensing methods. We also plotted the ASE without GZ but with perfect (ideal) knowledge of the $\eta_1, \ldots, \eta_m$ at the nodes and optimal channel access probabilities. This model is analyzed in [10] and represents the maximum achievable ASE without GZ. Besides, the ASE with separate optimization (first γ^* using (20), then θ^*) is also shown. One can observe that, although sensing is imperfect, large gains are obtainable through controlling self-interference using a GZ and through joint optimization over θ and γ.

In contrast to the ASE, the optimal thresholds θ^*, γ^* disclose the different behaviors of the three sensing methods as depicted in Fig. 6. While RSS and PER sensing show similar characteristics, this is not the case for CD. Unlike θ^*_r and θ^*_p, θ^*_c does not vary significantly over λ_b. Remarkably, the optimal thresholds θ_r and θ_p are of the same order, though they have different physical meanings. The latter holds for reasonably low ϵ. In particular, for $\epsilon \to 0$, $\theta_r = \theta_p$ which follows from considering (16a) and (16b) and noting that $\lambda_b \gamma^{\frac{2}{\alpha}} \to 0$ is a necessary condition for $\epsilon \to 0$. Furthermore, the difference in γ^* for the three sensing methods is insignificant.

C. Implications for protocol design

The optimal thresholds θ^* and γ^* are sensitive to the amount of self-interference, or equivalently, to the density of active transmitters, particularly at low target OPs. Especially in the regime where self-interference is present but does not dominate ($0.001 \leq \lambda_b \leq 0.1$ for typical WPAN/WLAN scenarios), large performance gains are obtainable, however, at the cost of adapting θ and γ. Among the different sensing techniques, CD sensing seems preferable since the range of the corresponding threshold is much smaller (< 5 dB) compared to PER and RSS sensing, and hence adaptation is practically not required. For very low target OPs, adaptation of the AFH threshold is generally not necessary. Although optimized PER requires the sensing threshold to be adapted to self-interference, it might be a good choice because sensing is *implicit*, i.e., it is carried out during data transfer and comes at no additional cost.

V. Conclusion

Practical AFH with imperfect sensing must not necessarily result in a performance loss: A cross-layer joint optimization over the AFH and GZ mechanisms can compensate for imperfect sensing. This has been shown by investigating the ASE for three commonly used sensing methods. CD sensing was found promising due to its inherent robustness against self-interference. With CD, practically no AFH threshold adaptation is needed. In contrast, RSS and PER sensing require threshold adaptation to maximize ASE. For low OPs, independent of the sensing technique, only the GZ threshold needs to be controlled which may simplify system design.

Acknowledgements

The authors gratefully acknowledge that their work is partially supported within the priority program 1397 "COIN" under grant No. JO 258/21-1 by the German Research Foundation (DFG).

References

[1] J. Andrews, S. Weber, and M. Haenggi, "Ad hoc networks: To spread or not to spread," *IEEE Commun. Magazine*, Dec 2007.

[2] A. Hasan and J. Andrews, "The guard zone in wireless ad hoc networks," *IEEE Trans. Wireless Commun.*, Mar 2007.

[3] "Part 15.2: Coexistence of wireless personal area networks with other wireless devices operating in unlicensed frequency bands," *IEEE Std 802.15.2-2003*, 2003.

[4] C. D. M. Condeiro and D. P. Agrawal, *Ad Hoc & Sensor Networks: Theory And Applications*. World Scientific Pub. Co. Inc., 2006.

[5] R. Tanbourgi, J. Elsner, H. Jäkel, and F. Jondral, "Adaptive frequency hopping in ad hoc networks with rayleigh fading and imperfect sensing," *IEEE Wireless Commun. Lett. (to appear)*, 2012.

[6] S. Weber, J. Andrews, and N. Jindal, "An overview of the transmission capacity of wireless networks," *IEEE Trans. Commun.*, Dec 2010.

[7] F. Baccelli and B. Blaszczyszyn, "Stochastic geometry and wireless networks, volume 1+2: Theory and applications," *Foundations and Trends in Networking*, 2009.

[8] A. Hunter, R. Ganti, and J. Andrews, "Transmission capacity of multi-antenna ad hoc networks with csma," in *Forty Fourth Asilomar Conf. on Signals, Systems and Computers (ASILOMAR)*, Nov. 2010.

[9] D. Stoyan, W. Kendall, and J. Mecke, *Stochastic geometry and its applications*, 2nd ed. Wiley, 1995.

[10] J. Elsner, R. Tanbourgi, and F. Jondral, "Hopping strategies for adaptive fh-cdma ad hoc networks under external interference," in *IEEE Int. Conf. on Commun. 2012*, Jun 2012.